


RESEARCH

Open Access



Air gap eccentric analysis and fault detection of traction motor

Jintian Yin^{1,2*} , Zhilong He^{1,2}, Li Liu^{1,2} and Zhihua Peng^{1,2}

*Correspondence:
yinjintian0115@163.com

¹ School of Electrical Engineering,
Shaoyang University,
Shaoyang 422000, China

² Hunan Provincial Key
Laboratory of Grids Operation
and Control On Multi-Power
Sources Area, Shaoyang
University, Shaoyang 422000,
China

Abstract

To solve the problem of air gap eccentric fault of traction motor, the fault characteristic frequency is close to the fundamental frequency, and the decomposed frequency affects each other, which is easy to cause spectrum aliasing. A reconstruction of variational mode decomposition method is proposed (reconstructed variational mode decomposition, RVMD); first of all, to construct and solve the variational stator current signal problem, to find the best decomposition number, and to obtain multiple modal functions, and to realize the effective separation and frequency profile of each component of the signal. Then, the decomposed modal function components with different frequencies and different amplitude can keep the decomposed positions unchanged and be reconstructed to form a new frequency spectrum. Experimental results show that the proposed RVMD method can detect weak faults timely and effectively, and has good application value.

Keywords: Fault detection, RVMD, Traction motor, Air gap eccentric

Introduction

The weak fault detection of traction motor is of great significance to ensure the safe operation of high-speed trains. Through the effective monitoring and diagnosis of the weak fault in the early stage of faults, it can prevent the further expansion of faults and prevent the occurrence of major accidents. Common types of traction motor fault include air gap eccentric fault, rotor fault, stator fault and bearing fault [1, 2].

About air gap eccentric fault detection of traction motor, Cameron deduced and verify from the traditional magnetoguide wave and magnetic motive force of the motor, some frequency-specific current components will appear in the stator current, which provides an effective method for detecting and studying the fault of the air gap [3]. Ceban A completed the air gap eccentric fault monitoring by establishing a neural network that maps the overlap area of the rotor and the air gap change under the air gap eccentric [4]. Hwang D H proposed a method by using radial magnetic flux sensor to compare the induced electromotive force waveform in healthy and eccentric states, and use this as the basis for detecting eccentric faults [5]. Ceban A proposed the axial magnetic flux change in the case of external magnetic field [6]. Seungdeog Choi, through the iterative analysis of multiple fault characteristic modes in the motor current signal proposed a

robust diagnostic technology for air gap eccentric fault detection. Under the conditions of high noise and nonlinear machine operation, it can not only ensure high monitoring accuracy, but also reduce the misdetection rate and leakage rate [7]. Jun-Kyu Park proposed a fault detection algorithm for the mixed short circuit, dynamic eccentric fault, and use a system matrix to diagnose and distinguish the fault types [8]. For the motor air gap eccentric fault diagnosis, different detection methods have been formed according to different diagnostic systems. Starting from the fault monitoring amount, it mainly includes current monitoring, magnetic field monitoring, voltage monitoring and vibration monitoring, among which the current monitoring mode is the most common. At present, the research on the motor air gap eccentric fault diagnosis is limited to the eccentric fault to a certain degree, and there are relatively few studies on the early eccentric fault diagnosis due to the difficulty in detecting and extracting the fault features.

In the early eccentric fault of traction motor, because the fault characteristic current is very weak, it is often submerged in the noise of the system operation, and the fault characteristic frequency is very close to the base frequency of the stator current, so the conventional detection method is often difficult to realize the detection well.

Variational mode decomposition (VMD) [9, 10] published in 2014 is a new signal processing method with good adaptability. It has the advantages of good noise robustness, high algorithm efficiency and no need for signal pretreatment in view of the good VMD denoising effect and no need to preprocess the signal. Because the fault characteristic frequency of the traction motor is close to the base frequency, the decomposed frequency affects each other, and the spectrum is easy to overlap, which causes the failure feature to appear, and the effect of directly using VMD for fault monitoring is not ideal. Therefore, this paper proposes a fault detection method based on the reconstructed variational mode decomposition (RVMD). This method constructs the variational problem of detection signal, and solves multiple modal functions. By superposition and reconstructing the modal function, the weak fault detection of traction motor air gap eccentric is well realized.

The content of this article is as follows: (1) principles analysis of air gap eccentric fault; (2) RVMD Introduction of the fault detection method; (3) weak fault detection of traction motors based on RVMD; (4) experimental validation of the proposed method.

Air gap eccentric fault

The long-term operation of the traction motor will wear the stator, rotor and bearing, or due to its own manufacturing error, there is a certain deviation between the motor rotor and the stator. The type of motor air gap eccentric mainly includes static eccentric and dynamic eccentric (as shown in Fig. 1), and the air gap eccentric will cause the motor electromagnetic vibration. Due to static eccentricity, a large unilateral magnetic tension is produced in the air gap. When the eccentricity is serious, even the rotor and rotors interact because the rotating magnetic field frequency passing through the minimum gas gap point is f_1/p . The rotor rotates for each week, the unbalanced magnetic tension will all change $2p$ time. Therefore, the vibration frequency and the unbalanced magnetic tension frequency caused by the static eccentricity are double $(f_1/p) \times 2p = 2f_1$. Its frequency is twice that of the power supply. When the dynamic eccentric is eccentric, the unbalanced mechanical force and electromagnetic force will be generated inside the

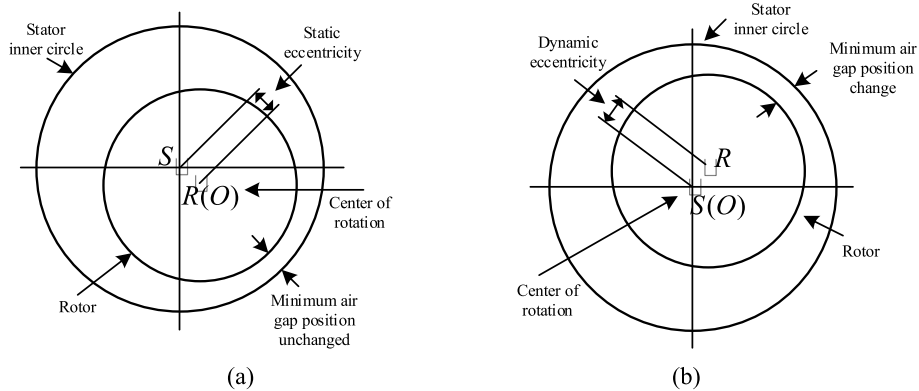


Fig. 1 The eccentric geometry model of the air gap: **a** static eccentricity; **b** dynamic eccentricity

motor, and the mechanical vibration will further have an adverse effect on the unbalanced electromagnetic force. The rotor velocity and the rotational magnetic field frequency are $(1 - s)f_1/p$ and f_1/p , respectively. The electromagnetic vibration frequency is f_1/p , and the pulsating in cycle $1/2sf_1$. When the motor load increases, the motor speed will decrease, the rotation rate will increase, and the pulsation will accelerate.

The general steps of eccentric fault mechanism analysis are as follows: first obtain the air gap magnetic potential, then calculate the air gap magnetic flux, and finally analyze the various harmonics in the stator current.

The harmonic frequency in the stator current can be calculated by the following equation [11]:

$$f_{ag} = \{(n_z z_2 \pm n_d) \frac{(1 - s)}{p} \pm n_s\} f_1 \tag{1}$$

Where f_1 is Power base frequency; n_z refers to any integer; Number of rotor slots z_2 ; n_d refers to any integer ($n_d = 0$ Quiet eccentric, $n_d = 1, 2, 3 \dots$ Move eccentric); Motor pole logarithm p ; revolutional slip; slip ratio s ; odd integer n_s .

Establish the characteristic frequency formula of air gap eccentric fault through electric field analysis:

$$f_{ag} = [n \pm k(1 - s)] f \tag{2}$$

Where $n = 1, 2, 3, \dots$, $k = 1/p, 2/p, \dots$. This equation is a special case of Eq. (1).

Reconstructed variational mode decomposition (RVMD)

The RVMD method uses the VMD to decompose the modal function, and then reconstruct the modal function by superposition in the frequency domain to obtain the reconstructed signal.

The acquisition of the mode function is divided into two steps: one is to construct the variational problem, and the other is to solve the structured variational problem.

The construction variational problem is to find multiple modal functions $u_k(t)$, so that the estimated bandwidth sum of each mode is the minimum, and the constraint is that the sum of each mode is equal to the original input signal y .

$$\begin{cases} \min_{\{u_k\}, \{\omega_k\}} \{ \sum_k \|\partial_t[(\delta(t) + \frac{j}{\pi t}) * u_k(t)]e^{-j\omega_k t}\|_2^2 \} \\ s.t. \sum_k u_k = y \end{cases} \tag{3}$$

Where $\{u_k\} = \{u_1, \dots, u_k\}$ is each set of modal functions. $\{\omega_k\} = \{\omega_1, \dots, \omega_k\}$ is the set of central frequencies corresponding to each mode u_k . ∂_t is a partial derivative of the time for a function; $\delta(t)$ is the unit pulse function and j is a virtual number unit; $*$ denotes convolution $\|\cdot\|_2^2$ shows the square of the L2 norm.

The variational problem is solved by the introduction of an augmented Lagrangian to turn the constrained variational problem into a non-constrained variational problem,

$$L(\{u_k\}, \{\omega_k\}, \lambda) := \alpha \sum_k \|\partial_t[(\delta(t) + \frac{j}{\pi t}) * u_k(t)]e^{-j\omega_k t}\|_2^2 + \|f(t) - \sum_k u_k(t)\|_2^2 + \langle \lambda(t), f(t) - \sum_k u_k(t) \rangle \tag{4}$$

Where α is secondary punishment factor. λ represents the Lagrange multiplication operator and $L(\cdot)$ represents a Lagrangian function. $\langle \cdot \rangle$ is Internal product operation.

Through the alternating direction method of multiplication operator, the component and center frequency are constantly updated to find the saddle point (optimal solution) of the above Lagrange function, and decompose the original input signal into K narrow-band eigenmode function components. The value of u_k^{n+1} can be expressed as follows:

$$u_k^{n+1} = \arg \min_{u_k \in X} \{ \alpha \|\partial_t[(\delta(t) + \frac{j}{\pi t}) * u_k(t)]e^{-j\omega_k t}\|_2^2 + \|f(t) - \sum_i u_i(t) + \frac{\lambda(t)}{2}\|_2^2 \} \tag{5}$$

Among $\omega_k = \omega_k^{n+1}$, $\sum_i u_i(t) = \sum_{i \neq k} u_i(t)^{n+1}$. (3)–(7) is Parseval/Plancherel changed to the frequency domain,

$$\hat{u}_k^{n+1} = \arg \min_{\hat{u}_k, u_k \in X} \{ \alpha \|j\omega[(1 + \text{sgn}(\omega + \omega_k)) * \hat{u}_k(\omega + \omega_k)]\|_2^2 + \|\hat{f}(\omega) - \sum_i \hat{u}_i(\omega) + \frac{\hat{\lambda}(\omega)}{2}\|_2^2 \} \tag{6}$$

Change ω of the first term in (6) to $\omega - \omega_k$ and change it to the integral form of the non-negative frequency interval,

$$\hat{u}_k^{n+1} = \arg \min_{\hat{u}_k, u_k \in X} \{ \int_0^\infty 4\alpha(\omega - \omega_k)^2 |\hat{u}_k(\omega)|^2 d\omega + 2 \left| \hat{f}(\omega) - \sum_i \hat{u}_i(\omega) + \frac{\hat{\lambda}(\omega)}{2} \right|^2 d\omega \} \tag{7}$$

Find the solution of the secondary optimization problem,

$$\hat{u}_k^{n+1}(\omega) = \frac{\hat{f}(\omega) - \sum_{i \neq k} \hat{u}_i(\omega) + \frac{\hat{\lambda}(\omega)}{2}}{1 + 2\alpha(\omega - \omega_k)^2} \tag{8}$$

The value problem of the central frequency can also be converted to the frequency domain,

$$\omega_k^{n+1} = \arg \min_{\omega_k} \left\{ \int_0^\infty (\omega - \omega_k)^2 |\hat{u}_k(\omega)|^2 d\omega \right\} \tag{9}$$

The results of the central frequency calculation are shown in (10):

$$\omega_k^{n+1} = \frac{\int_0^\infty \omega |\hat{u}_k(\omega)|^2 d\omega}{\int_0^\infty |\hat{u}_k(\omega)|^2 d\omega} \tag{10}$$

Inside, $\hat{\omega}_k^{n+1}(\omega)$ Wiener filter equivalent to $\hat{f}(\omega) - \sum_{i \neq k} \hat{u}_i(\omega)$. ω_k^{n+1} is the center of gravity of the power spectrum of the current mode function. Perform the inverse Fourier transform of $\{\hat{u}_k(\omega)\}$, which is actually the part of $\{u_k(t)\}$.

Through the above steps to find the best decomposition number, also obtained the specific parameters of each component, realize the effective separation of signal components and frequency profile, but the traction motor weak fault frequency and base frequency is very close, which results in the decomposition of the component frequency spectrum overlap phenomenon and affects the embodiment of the fault characteristics. Therefore, the next step is to keep the decomposition of the modal function components with different frequencies and different amplitude at the decomposed positions unchanged, and to reconstruct them according to (11) to form a new frequency spectrum.

$$f_{rec} = \sum_{i=1}^K u_i + r_K \tag{11}$$

Where u_i and r_K are the modal function components and residual terms, respectively, and the noise component is filtered out in the new spectrum.

Weak fault detection of traction motors based on RVMD

RVMD process

The weak fault detection method of traction motor based on RVMD is composed of three parts: variational problem construction, mode function solution, and mode function component superposition reconstruction and fault detection decision. The specific implementation process is as follows:

- (1) Load the original stator current signal y to construct the variational problem, y including the base frequency, fault component and noise;
- (2) Initialize $\{u_k^1\}$, $\{\omega_k^1\}$, λ^1 , n is 0;
- (3) $n = n + 1$, Perform the entire cycle;
- (4) Update u_k according to (8), execute the first inner cycle;
- (5) $k = k + 1$, Repeat steps (4), until $k = K$, when the first loop of the inner layer ends;
- (6) Update ω_k according to (10), execute the second inner cycle;
- (7) $k = k + 1$, Repeat steps (6), Until $k = K$, the second cycle of the inner layer ends;
- (8) Update λ as per $\hat{\lambda}^{n+1}(\omega) \leftarrow \hat{\lambda}^n(\omega) + \tau [\hat{f}(\omega) - \sum_k \hat{u}_k^{n+1}(\omega)]$;

- (9) Repeat steps (3)~(8), the discrimination accuracy $\varepsilon > 0$, If $\sum_k \left\| \hat{u}_k^{n+1} - \hat{u}_k^n \right\|_2^2 / \left\| \hat{u}_k^n \right\|_2^2 < \varepsilon$, end the whole cycle and output K IMF components, otherwise return to step (3);
- (10) Reconstruct the output K modal function components according to formula (11) to realize the weak fault detection of traction motor;
- (11) Make the corresponding fault detection decision according to the reconstruction signal.

The step (1) is the variational problem construction. The step (2)~(9) is the modal function according to the variational problem. The step (10) is the modal function component superposition reconstruction. The step (11) is the fault detection decision.

RVMD parameter

The main parameters included in the RVMD algorithm are discriminant accuracy ε , noise tolerance τ , decomposition scale K , and penalty factor α . Specifically, the relative decomposition scale and the penalty factor of the discrimination accuracy and the noise tolerance have less influence on the RVMD output results. Therefore, this paper focuses on the selection of decomposition scale K and penalty factor α , while the discrimination accuracy and noise tolerance often adopt the standard VMD decomposition default value.

Selection of the decomposition scale K

Before decomposition, the value of decomposition scale K is determined. If the K is small, the number of components is small, and if the K is large, the number of components is large. The less or more decomposition number is not conducive to the decomposition effect, in which the decomposition number will filter out part of the starting signal information, and the decomposition number will make the central frequency band of the decomposed component overlap. Therefore, the value of the decomposition scale K can be determined by trying to gather together the method:

- 1) Input the original signal;
- 2) The decomposition scale K was set to 2, and the penalty factor, discriminant accuracy, and noise tolerance were set to the standard VMD decomposition default values, respectively, $\alpha=2000$, $\varepsilon=1.0 \times 10^{-7}$, $\tau=0$;
- 3) According to the above parameters to achieve the input signal decomposition and the frequency spectrum of each component;
- 4) Check whether the center frequencies in the spectrum overlap; if no overlap occurs, make $K = K + 1$, return to step 3 to continue VMD decomposition, otherwise output $K = K - 1$. If center frequency overlap occurs at $K = 2$, increase K value until no overlap occurs, and then follow the no overlap step.

Selection of the punishment factor α

Introducing the penalty factor transforms the variational problem from the constraint to non-constraint condition, which mainly affects the convergence rate and bandwidth of the decomposition component.

Experimental

Experimental platform

In the established dSPACE hardware realizes the weak fault injection of the traction motor on the ring semi-physical platform of the CRH2 EMU traction drive system, the references [12–14] gives a detailed introduction, and the fault injection simulation platform can be downloaded on the website <http://gfist.csu.edu.cn/indexE.html>. The experimental device used here included a dSPACE-based CRH2 EMU traction drive control system controller in the loop real-time fault semi-physical platform (Fig. 2).

Selection of the RVMD parameters

Decomposition scale K

Through the analysis of the important parameters of RVMD in “Reconstructed variational mode decomposition (RVMD)” section, the original signal is decomposed with different K values. The other parameters are $\alpha=2000$, $\varepsilon=1.0 \times 10^{-7}$, $\tau=0$, and the central frequency change curve during the decomposition of RVMD is shown in Fig. 3.

We can find from Fig. 3, when $K=2$, the decomposition results are shown in Fig. 3a, and the center frequencies of the two components of the signal decomposition overlap;

When $K=3$, the decomposition results are shown in Fig. 3b. The three components of the signal decomposition do not overlap each other and contain all the characteristic frequency band information of the original signal.

When $K=4$, the decomposition results are shown in Fig. 3c. Although the four components of the signal decomposition are not overlapping, they are close to each other.

Further increase of the K . When $K=5$, the decomposition result is shown in Fig. 3d, and the central frequency of the decomposition component appears seriously stacked in the high frequency part.

Therefore, Consider the aliasing problem between signal decomposition components and center frequency, we can select $K=3$.

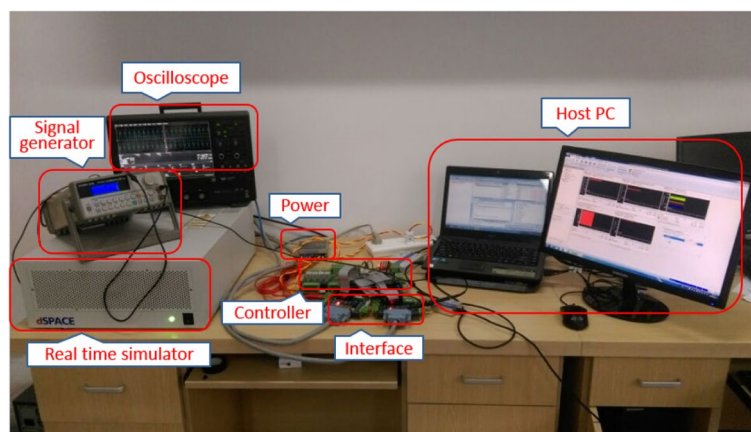


Fig. 2 Semi-physical platform of the CRH2 EMU traction drive system

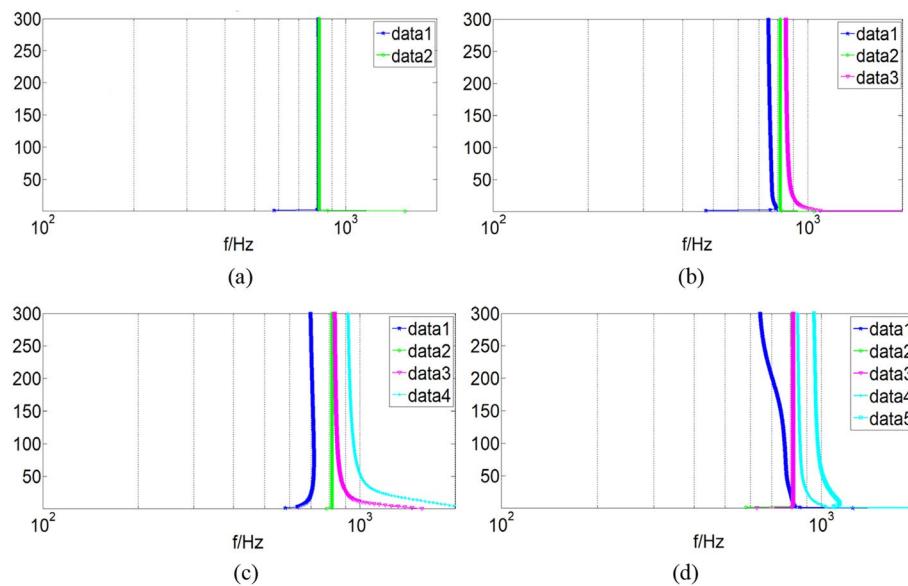


Fig. 3 Change curve of the center frequency: **a** $K=2$, $\alpha=2000$; **b** $K=3$, $\alpha=2000$; **c** $K=4$, $\alpha=2000$; **d** $K=5$, $\alpha=2000$

Penalty factor α

Different penalty factors are used to decompose the original signal. The decomposition scale value is 3, and the penalty factor is taken from 100 to 12,800. The decomposition results under different penalty factors are shown in Fig. 4, where the abscissa represents the center frequency of the decomposition component, and the overlapping or close separation indicates that the decomposition effect is not good.

1) Punishment factor of 100

The central frequency map shows that the high frequency component contains two components simultaneously, causing serious modal aliasing.

2) The penalty factor of 200–1600

When the penalty factor varies in this range, the mode stacking phenomenon is still very serious, and the VMD cannot decompose the modes of different central frequencies.

3) Punishment factor of 3200–12,800

When the penalty factor changes in this range, although the mode mixture appears, the component center frequency gets closer and closer as the penalty factor increases.

Therefore, it is found that the smaller the value of α , the more likely it is to overlap; with the increase of α , the decomposition effect of RVMD is better, but the value of α is not too large, and the center frequency of the modal component will be close.

Meanwhile, the change in the penalty factor α also has an effect on the calculation time of the RVMD program. Table 1 reflects the relationship between the two, which shows that the RVMD procedure takes less time to take the range from 400 to 6400, so the penalty factor α usually takes this range, and the shortest time is required for 800.

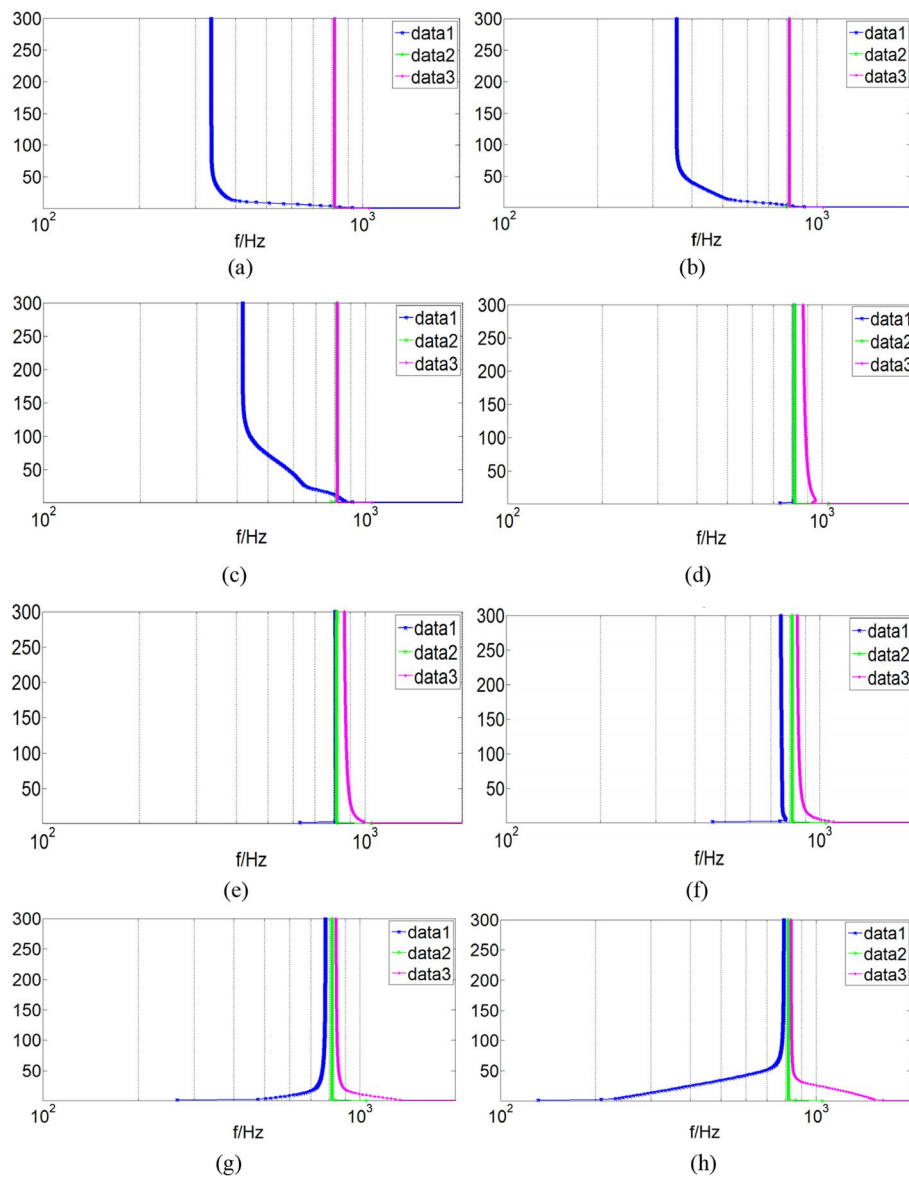


Fig. 4 Center frequency plot of each component at different values under the same value: **a** $K=3, \alpha=100$; **b** $K=3, \alpha=200$; **c** $K=3, \alpha=400$; **d** $K=3, \alpha=800$; **e** $K=3, \alpha=1600$; **f** $K=3, \alpha=3200$; **g** $K=3, \alpha=6400$; **h** $K=3, \alpha=12800$

Table 1 Effect of penalty factor on calculation time

Penalty factor α	RVMD run time
100	12.574
200	5.368
400	2.818
800	2.681
1600	2.709
3200	2.735
6400	2.784
12,800	2.932

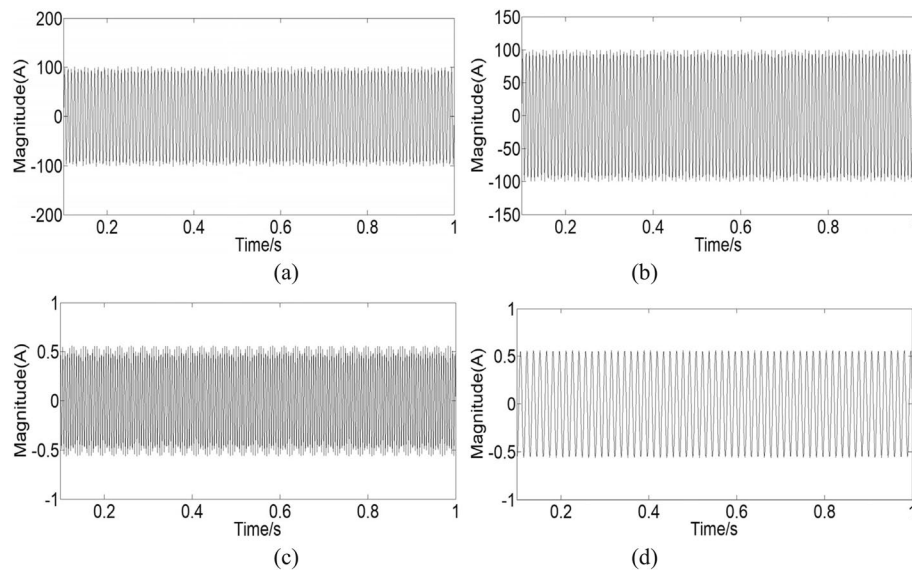


Fig. 5 Current time-domain waveform: **a** total current time-domain waveform; **b** component 1 time-domain waveform; **c** component 2 time-domain waveform; **d** component 3 time-domain waveform

Therefore, considering the decomposed central frequency distribution and the RVMD running time, the selection of $\alpha = 2000$ for RVMD is highly reasonable. In this paper, the penalty factor α is taken at 2000 when using RVMD to decompose the weak fault signal of the traction motor.

Results and discussion

The degree of complete eccentric fault of visual air gap is 1, and the degree of air gap eccentric fault is 0.002, 0.0056, and 0.012 on the semi-physical platform, respectively, to simulate the weak fault of eccentric air gap.

Figure 5a shows the current waveform of the air gap eccentric fault at 0.0056. Figure 5b–d shows the three components time-domain waveforms of the RVMD decomposed with the decomposition scale $K=3$. Directly observing the nos. 2, 3, and 4 components of stator current RVMD decomposition under different fault degrees, the difference is not obvious, and it is difficult to detect the weak fault of air gap eccentric.

The RVMD parameter selection is consistent with the first two weak failures, namely $K=3$, $\alpha=2000$, $\varepsilon=1.0 \times 10^{-7}$, and $\tau=0$. Figure 6 shows the stator A phase current frequency spectrum under different weak degrees of failure. Numbers. 2, 3, and 4 are the main component spectrum of phase A current RVMD decomposition, and no. 1 is the superimposed reconstructed frequency spectrum (RVMD spectrum) of no. 2, 3, and 4 components.

Observing the frequency spectrum no. 1 after RVMD can determine whether a malfunction has occurred and the severity of the malfunction. Figure 6a shows no fault, and the A phase current spectrum no. 1 has no fault component on either side of the vertical line; even in the early weak fault Fig. 6b, the fault component on both sides; the amplitude of fault component in Fig. 6c, d gradually increases and is larger than that in Fig. 6b, indicating that the weak fault of the air gap is more serious.

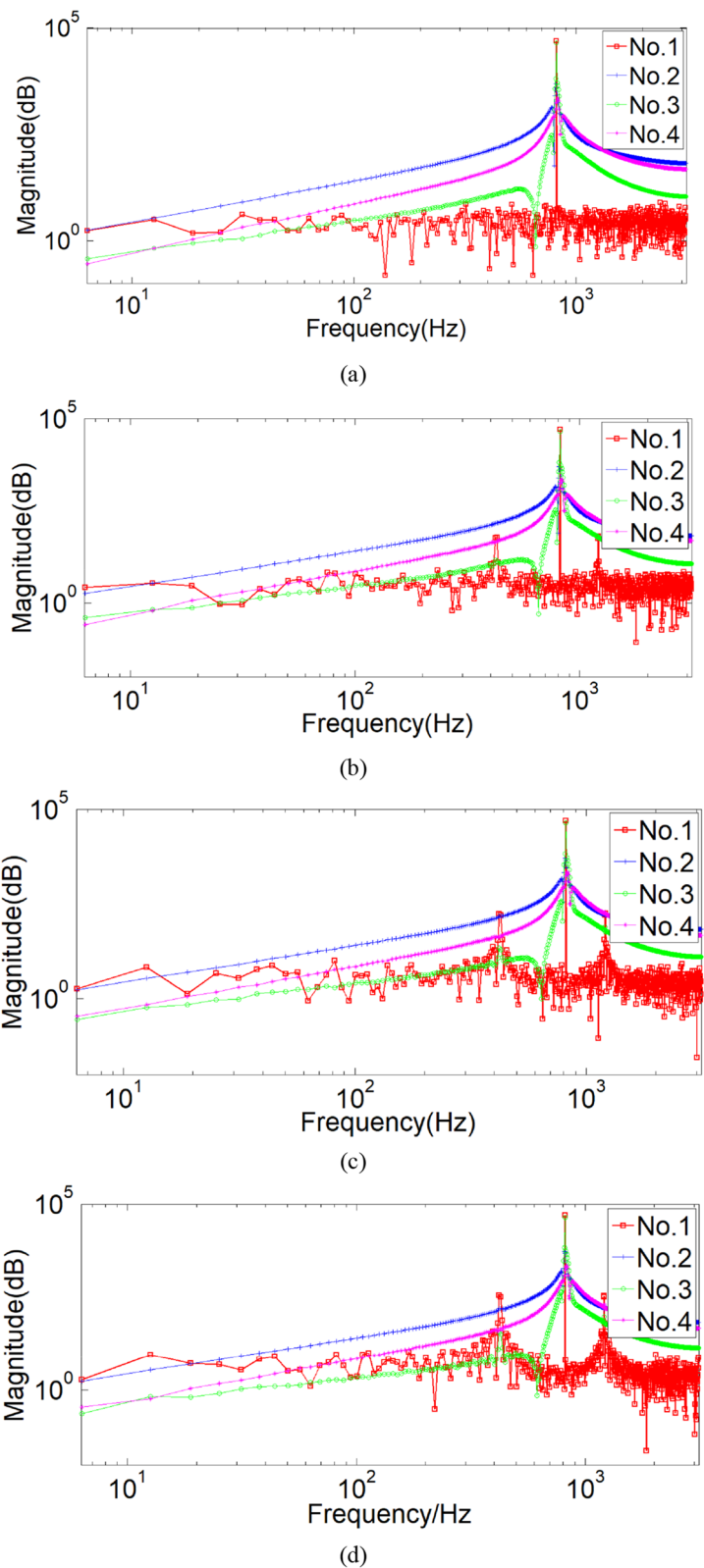


Fig. 6 The A-phase current RVMD spectrum at each degree of failure: **a** regular; **b** fault severity 0.002; **c** fault severity 0.0056; **d** fault severity 0.012

The above results show that the RVMD method can effectively detect weak faults in the air gap eccentric of traction motors by observing the fault components and their amplitude.

Comparison with existing methods

The method proposed in the introduction is mainly used for detecting air gap eccentric to a certain extent after the fault occurs and is not suitable for detecting weak faults. Moreover, the proposed RVMD method has high efficiency and good operability, and performs better than traditional methods such as EMD and VMD in detecting weak faults in the air gap eccentric of traction motors.

Conclusions

This article proposes a signal decomposition and reconstruction RVMD method based on the VMD method to address the issues of unclear changes in electrical parameters and frequency aliasing between fault characteristic frequencies and stator current fundamental frequencies in the case of weak faults in traction motors. By reasonably selecting important parameters such as decomposition scale and penalty factor, the detection signal is constructed and solved through variational problems, achieving effective separation of signal components and frequency partitioning; Then, the decomposed different modal components are superimposed and reconstructed to form a new spectrum, ultimately achieving weak fault detection. The proposed method has effectively achieved weak fault detection of air gap eccentric on the semi-physical platform of the traction transmission control system. At the same time, this method can also be used for detecting weak faults such as broken rotor bars, inter turn short circuits, and bearings in traction motors.

Abbreviations

RVMD	Rs
VMD	Variational mode decomposition

Acknowledgements

Not applicable.

Authors' contributions

All authors edited the manuscript and provided some references. All authors reviewed the results and approved the final version of the manuscript.

Funding

The research is supported by: Hunan Natural Science Foundation Project (2023JJ50270, 2023JJ50267); Hunan Education Department Youth Project (21B0690); Hunan Science and Technology Department Science and Technology Project (2016TP1023); Shaoyang Science and Technology Plan Project (2022GZ3034).

Availability of data and materials

All presented data are available under any request.

Declarations

Competing interests

The authors declare that they have no competing interests.

Received: 11 January 2023 Accepted: 10 June 2023

Published online: 23 June 2023

References

1. Rocio ALM, Carlos RD, Eduardo CY (2017) Novel FPGA-based methodology for early broken rotor bar detection and classification through homogeneity estimation. *IEEE T Instrum Meas* 66(7):1760–1769. <https://doi.org/10.1109/TIM.2017.2664520>
2. Rubino S, Mandrile F, Armando E et al (2022) Fault-tolerant torque controller based on adaptive decoupled multi-stator modeling for multi-three-phase induction motor drives. *IEEE T Ind Appl* 58(6):7318–7335. <https://doi.org/10.1109/TIA.2022.3197547>
3. Cameron JR, Thomson WT, Dow AB (1986) Vibration and current monitoring for detecting airgap eccentricity in large induction motors. *IET Electr Power App* 133(3):155–163. <https://doi.org/10.1049/ip-b.1986.0022>
4. Miller TJE (1995) Faults and unbalanced forces in the switched reluctance machine. *IEEE T Ind Appl* 31(2):319–328. <https://doi.org/10.1109/28.370280>
5. Hwang DH, Han SB, Woo BC et al (2008) Detection of air-gap eccentricity and broken-rotor bar conditions in a squirrel-cage induction motor using the radial flux sensor. *J Appl Phys* 103(7):07F131. <https://doi.org/10.1063/1.2839347>
6. Ceban A, Pusca R, Romary R (2012) Study of rotor faults in induction motors using external magnetic field analysis. *IEEE T Ind Electron* 59(5):2082–2093. <https://doi.org/10.1109/TIE.2011.2163285>
7. Seungdeog C, Elham P, Jeehoon B et al (2015) Iterative condition monitoring and fault diagnosis scheme of electric motor for harsh industrial application. *IEEE T Ind Electron* 62(3):1760–1769. <https://doi.org/10.1109/TIE.2014.2361112>
8. Park JK, Hur J (2016) Detection of inter-turn and dynamic eccentricity faults using stator current frequency pattern in IPM-type BLDC motors. *IEEE T Ind Electron* 63(3):1771–1780. <https://doi.org/10.1109/TIE.2015.2499162>
9. Konstantin D, Dominique Z (2014) Variational mode decomposition. *IEEE T Signal Proces* 62(3):531–544. <https://doi.org/10.1109/TSP.2013.2288675>
10. Liu SS, Yu KP (2022) Successive multivariate variational mode decomposition. *Multidim Syst Sign P* 33(3):917–943
11. Zhang HL, Wang YC, Hua W et al (2022) Analysis of the flux density and back EMF in eccentric permanent magnet machines based on 2-D air-gap modulation theory. *IEEE T Transp Electr* 8(4):4325–4336. <https://doi.org/10.1109/TTE.2022.3190728>
12. Yang XY, Yang CH, Peng T et al (2018) Hardware-in-the-loop fault injection for traction control system. *IEEE J Em Sel Top P* 6(2):696–706. <https://doi.org/10.1109/JESTPE.2018.2794339>
13. Yin JT, Xie YF, Peng T (2018) Current characteristics analysis and fault injection of an early weak fault in broken rotor bar of traction motor. *Math Probl Eng* 2018:1–8. <https://doi.org/10.1155/2018/4934720>
14. Yin JT, Xie YF, Chen ZW et al (2020) Fault tracing method based on fault propagation and causality with its application to the traction drive control system. *JAS* 46(1):47–57. <https://doi.org/10.16383/j.aas.c190257>

Publisher's Note

Springer Nature remains neutral with regard to jurisdictional claims in published maps and institutional affiliations.

Submit your manuscript to a SpringerOpen[®] journal and benefit from:

- Convenient online submission
- Rigorous peer review
- Open access: articles freely available online
- High visibility within the field
- Retaining the copyright to your article

Submit your next manuscript at ► [springeropen.com](https://www.springeropen.com)
